ADVANCED SCIENCE
Open Access

Supporting Information

for *Adv. Sci.*, DOI 10.1002/advs.202307029

In Situ Synthesis of Ru/TiO_{2-x}@TiCN Ternary Heterojunctions for Enhanced Sonodynamic and Nanocatalytic Cancer Therapy

Yin Zhao, Bo Yuan, Lang Yan, Zhiwei Wang, Zheng Xu, Bijiang Geng, Xiang Guo* and Xiongsheng Chen**

In-Situ Synthesis of Ru/TiO_{2-x}@TiCN Ternary Heterojunctions for Enhanced Sonodynamic and Nanocatalytic Cancer Therapy

Yin Zhao, Bo Yuan, Lang Yan, Zhiwei Wang, Zheng Xu, Bijiang Geng, Xiang Guo*, Xiongsheng Chen**

Y. Zhao, B. Yuan, Z. Wang, Z. Xu, X. Guo, X. Chen

Spine Center, Department of Orthopedics, Shanghai Changzheng Hospital, Naval Medical University, Shanghai, 200003, China

E-mail: gx9601074@smmu.edu.cn (X. Guo), cxspine@smmu.edu.cn (X. Chen)

L. Yan

Department of Health Toxicology, Faculty of Naval Medicine, Naval Medical University, Shanghai, 200433, China

B. Geng

School of Environmental and Chemical Engineering, Shanghai University, Shanghai 200444, China

E-mail: bjgeng1992@shu.edu.cn (B. Geng)

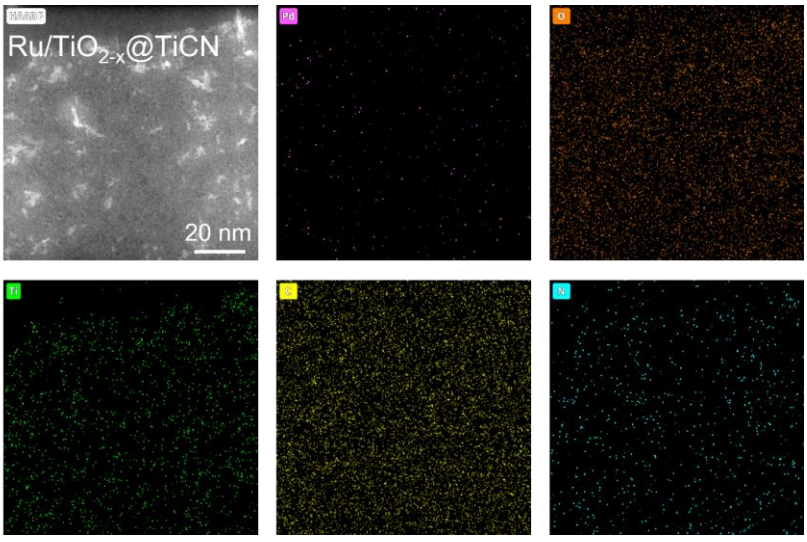

Figure S1. TEM element mapping images of Ru/TiO_{2-x}@TiCN.

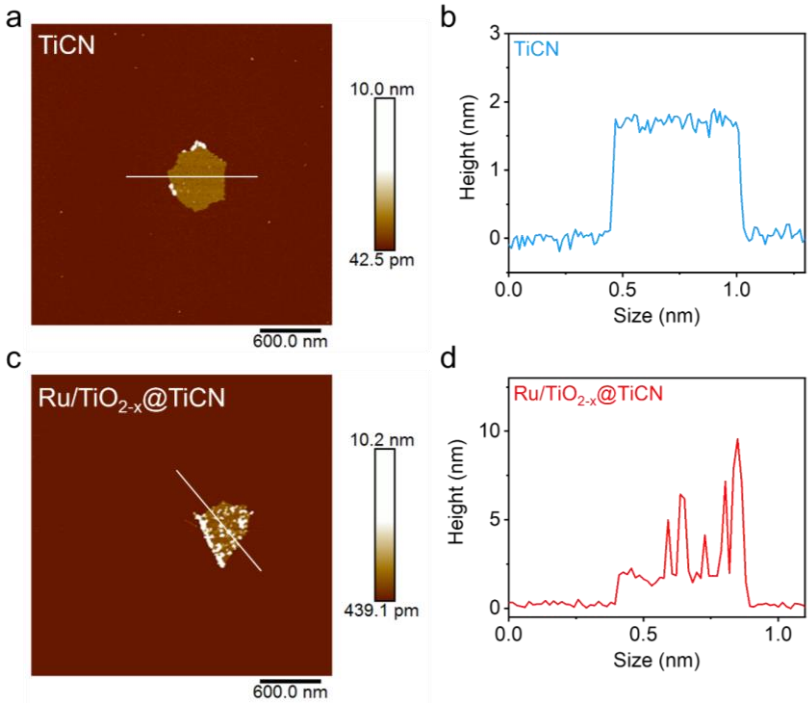

Figure S2. AFM image and displaying height profiles of TiCN (a, b) and Ru/TiO_{2-x}@TiCN (c, d).

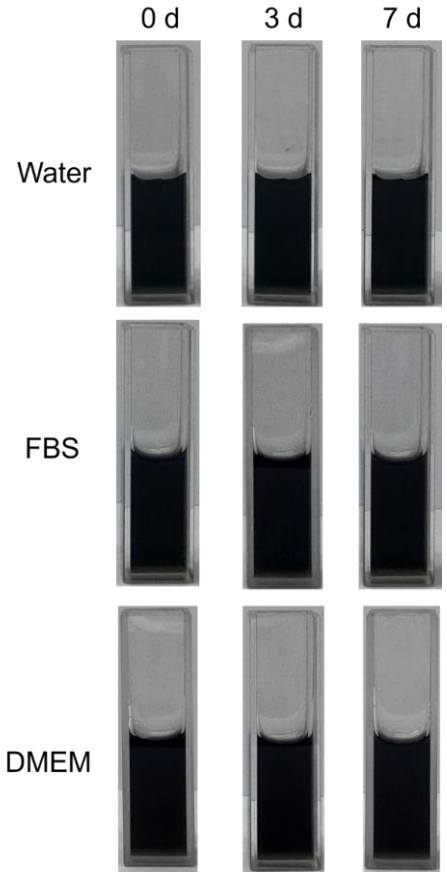

Figure S3. Photographs of Ru/TiO_{2-x}@TiCN aqueous solution, FBS solution, and DMEM solution stored for different periods of time (0, 3, and 7 days).

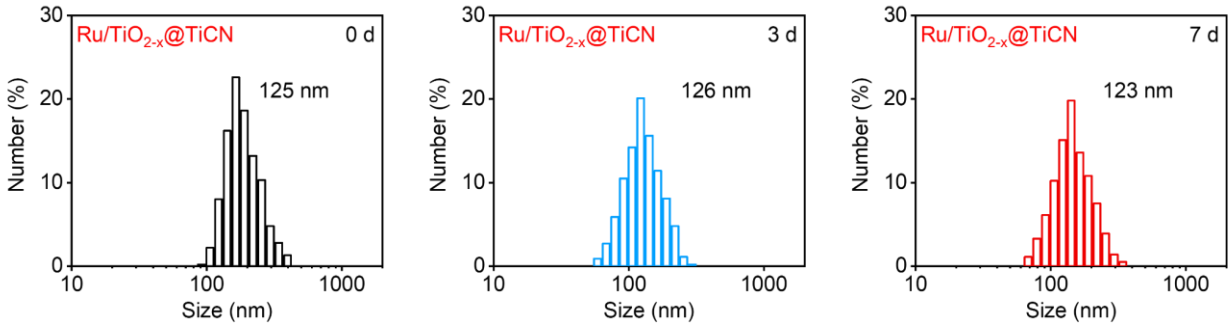

Figure S4. The hydrodynamic diameters of Ru/TiO_{2-x}@TiCN aqueous solution stored for 0, 3, and 7 days.

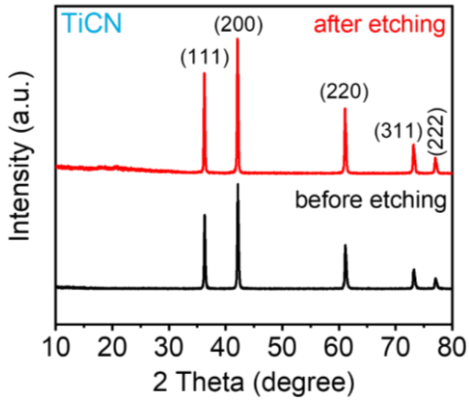

Figure S5. XRD patterns of TiCN before and after HF etching.

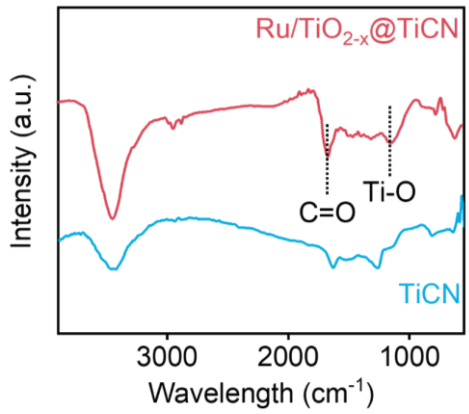

Figure S6. FTIR spectra of Ru/TiO_{2-x}@TiCN and TiCN.

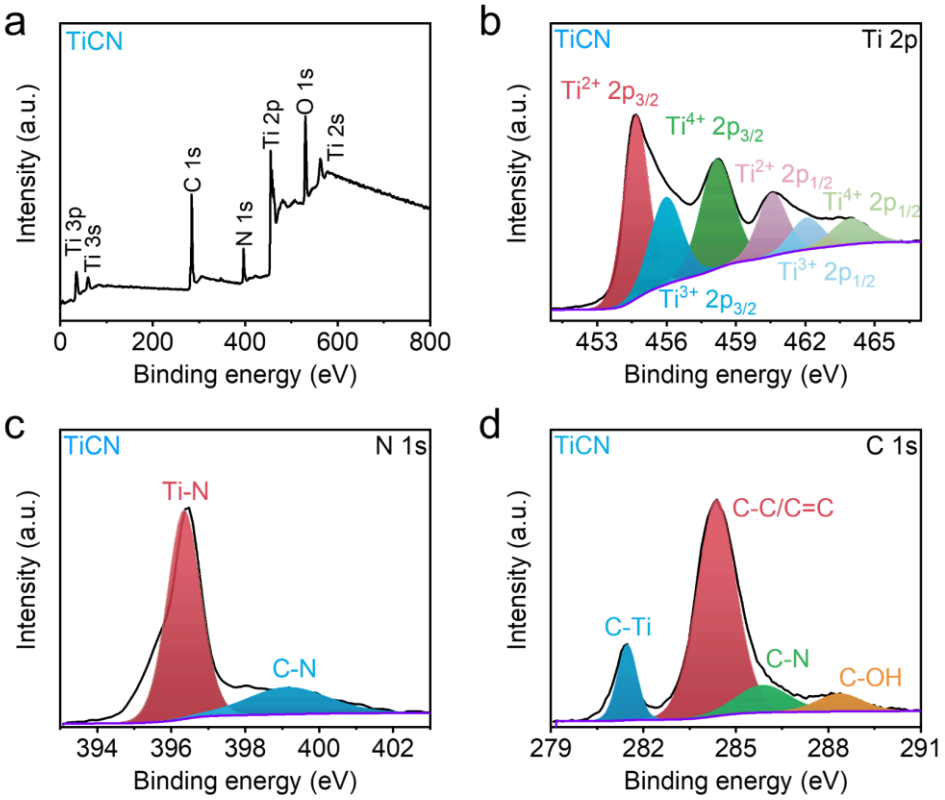

Figure S7. (a-d) The survey XPS (a), high-resolution Ti 2p (b), N 1s (c), and C 1s spectra (d) of TiCN NSs.

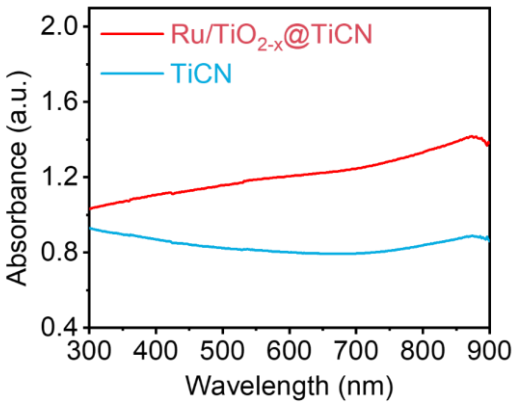

Figure S8. Absorption spectra of Ru/TiO_{2-x}@TiCN and TiCN.

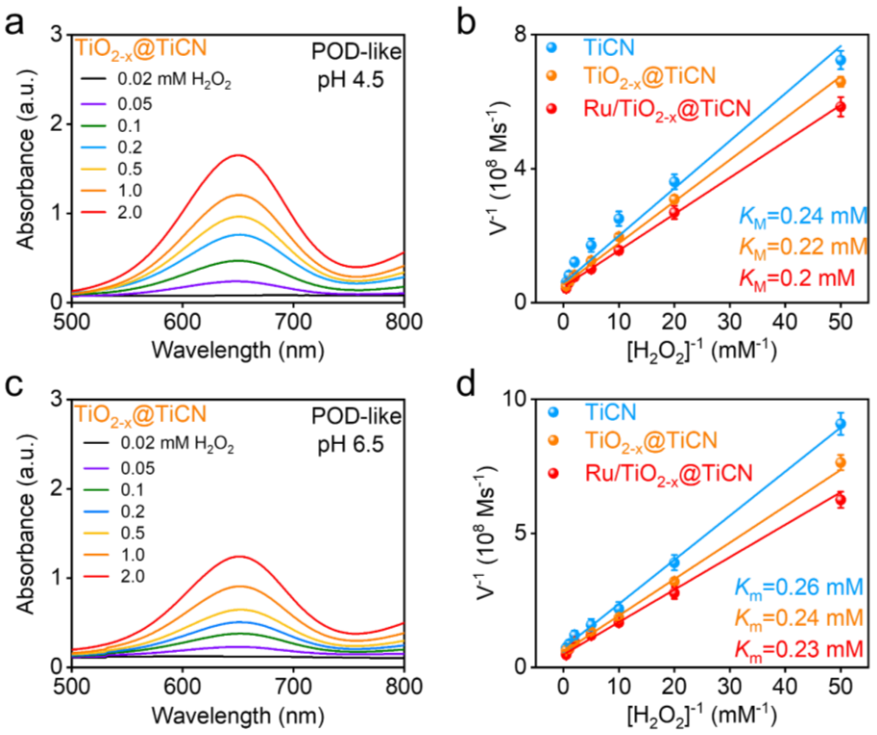

Figure S9. (a, c) Absorption change of TMB solution incubated with TiO_{2-x}@TiCN in the presence of H_2O_2 with varied concentration at pH 4.5 (a) and 6.5 (c). (b, d) Comparison of POD-like catalytic activity of Ru/TiO_{2-x}@TiCN, TiO_{2-x}@TiCN, and TiCN at pH 4.5 (b) and 6.5 (d).

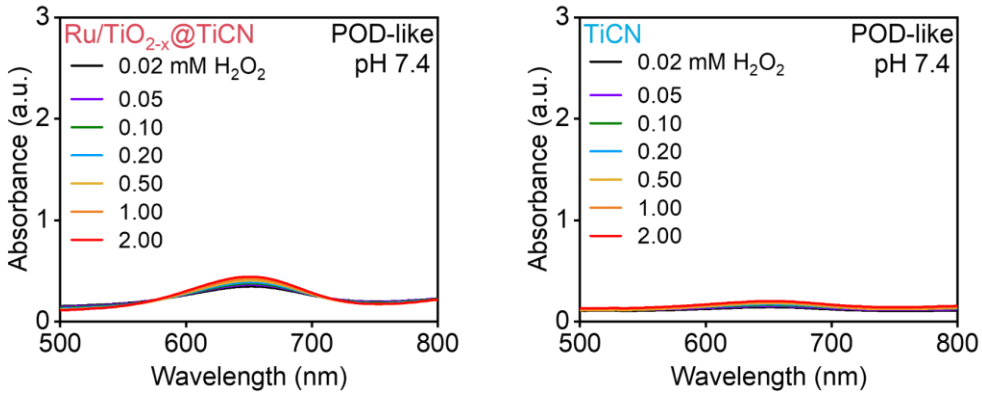

Figure S10. Absorption spectra of the oxidized TMB catalyzed by Ru/TiO_{2-x}@TiCN or TiCN at pH 7.4.

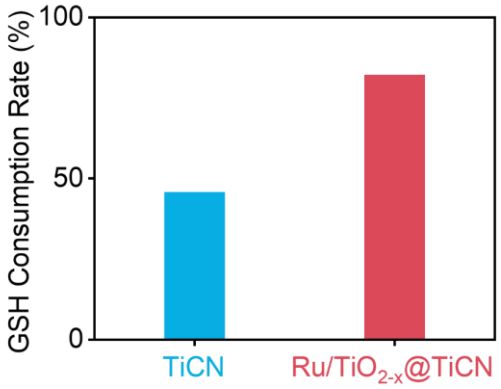

Figure S11. The GSH depletion activity evaluation of Ru/TiO_{2-x}@TiCN and TiCN.

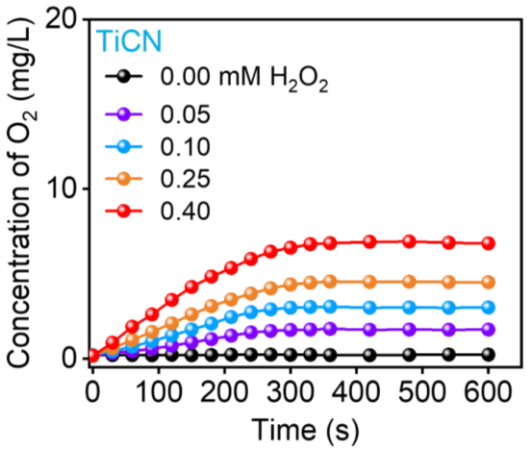

Figure S12. O_2 generation upon the addition of TiCN (0.4 mg/mL) in the presence of H_2O_2 with varied concentrations at pH 4.5.

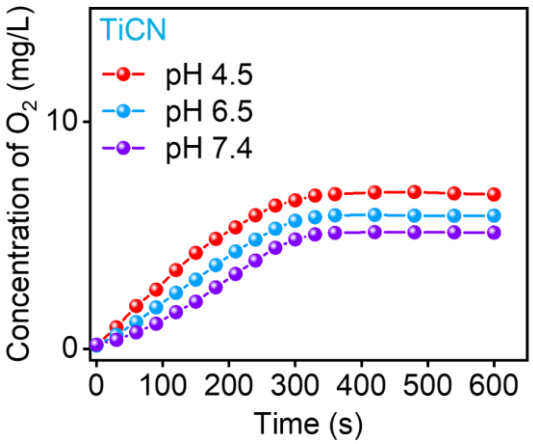

Figure S13. O_2 generation upon the addition of TiCN (0.4 mg/mL) and H_2O_2 (0.40 mM) at varied pH (4.5, 6.5, or 7.4).

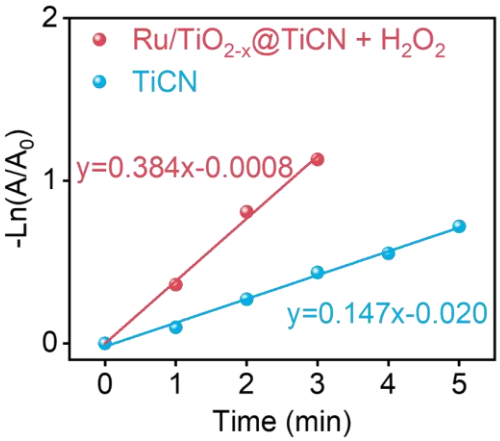

Figure S14. The rate constant of $^1O_2$ generation of Ru/TiO_{2-x}@TiCN and TiCN under US irradiation in the presence of H_2O_2 (0.40 mM).

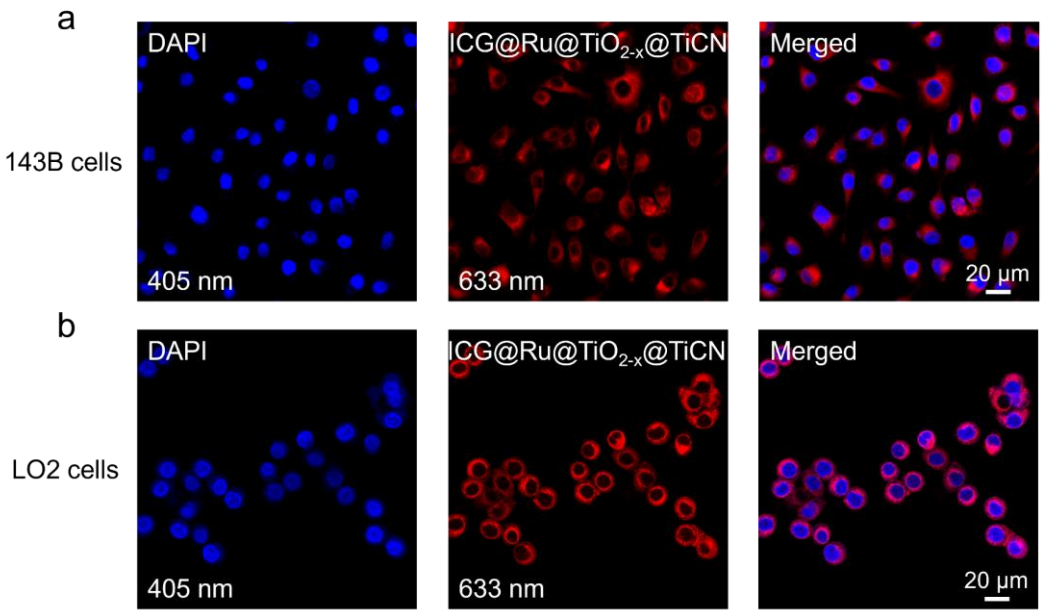

Figure S15. DAPI and ICG staining of 143B (a) or LO2 cells (b) incubated with ICG-labeled Ru/TiO_{2-x}@TiCN.

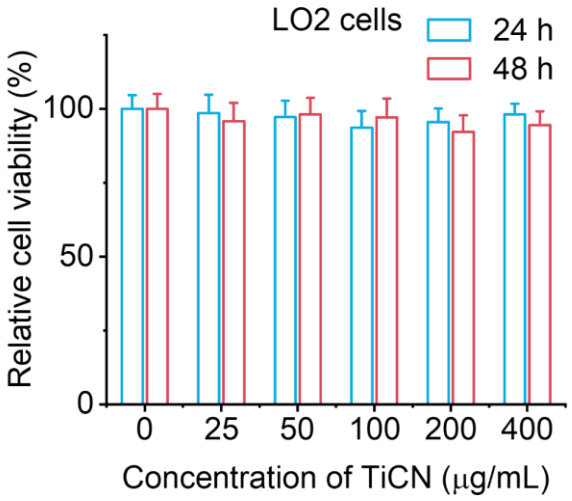

Figure S16. Relative cell viabilities of LO2 cells incubated with TiCN with varied concentrations for 24 or 48 h (n=6).

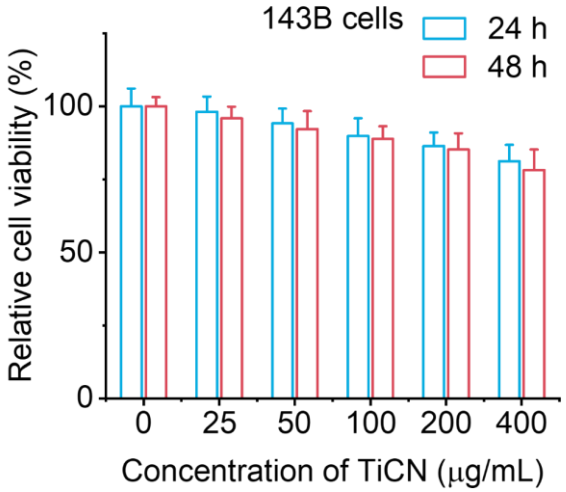

Figure S17. Relative cell viabilities of 143B cells incubated with TiCN with varied concentrations for 24 or 48 h (n=6).

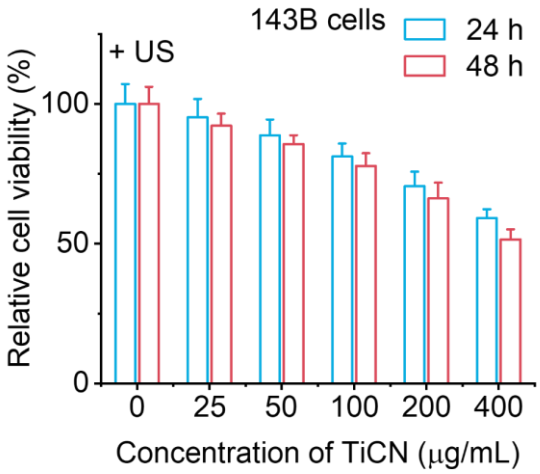

Figure S18. Relative cell viabilities of 143B cells incubated with TiCN with varied concentrations for 24 or 48 h in the presence of US irradiation (n=6).

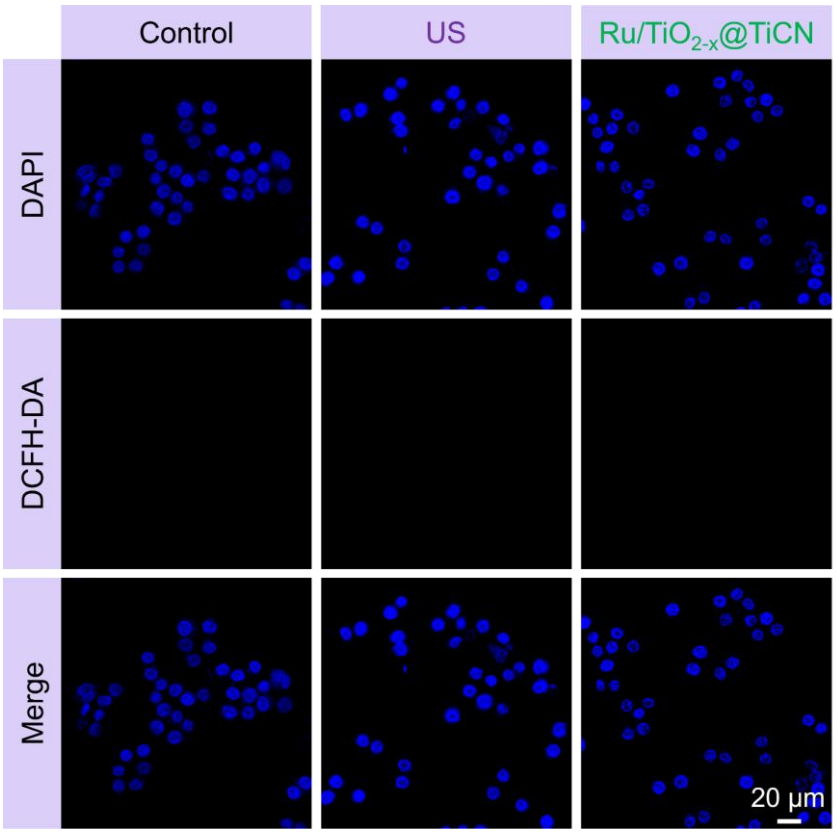

Figure S19. ROS staining of LO2 cells after different treatments.

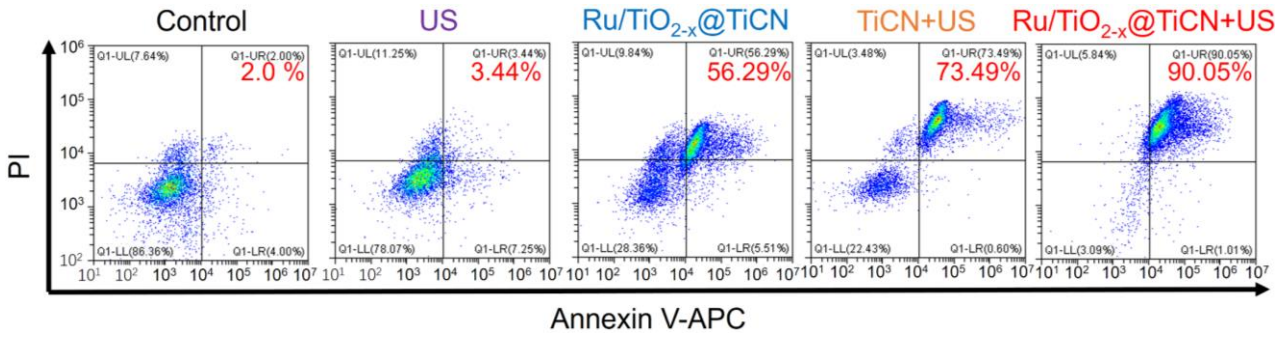

Figure S20. Flow cytometry apoptosis assay of 143B cells after different treatments.

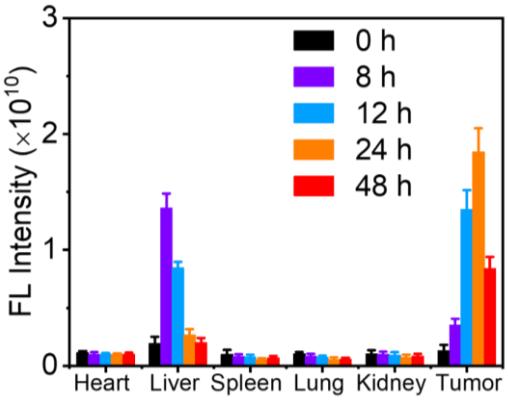

Figure S21. Time-dependent NIR fluorescence intensity of ICG-labeled Ru/TiO_{2-x}@TiCN in the major organs and tumor tissues based on the fluorescence imaging results (n=5).

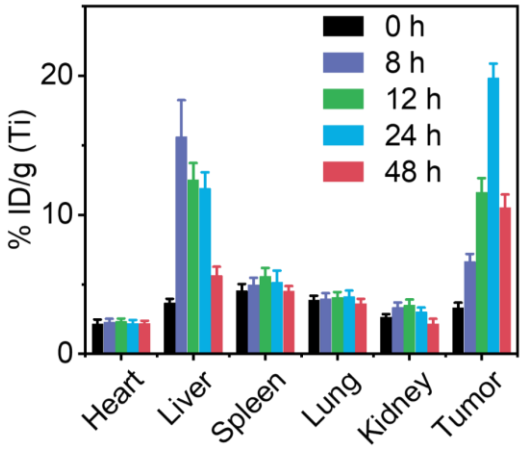

Figure S22. Biodistribution measurements of Ru/TiO_{2-x}@TiCN in major organs and tumors after intravenous injection of different times determined by ICP-MS (n=5).

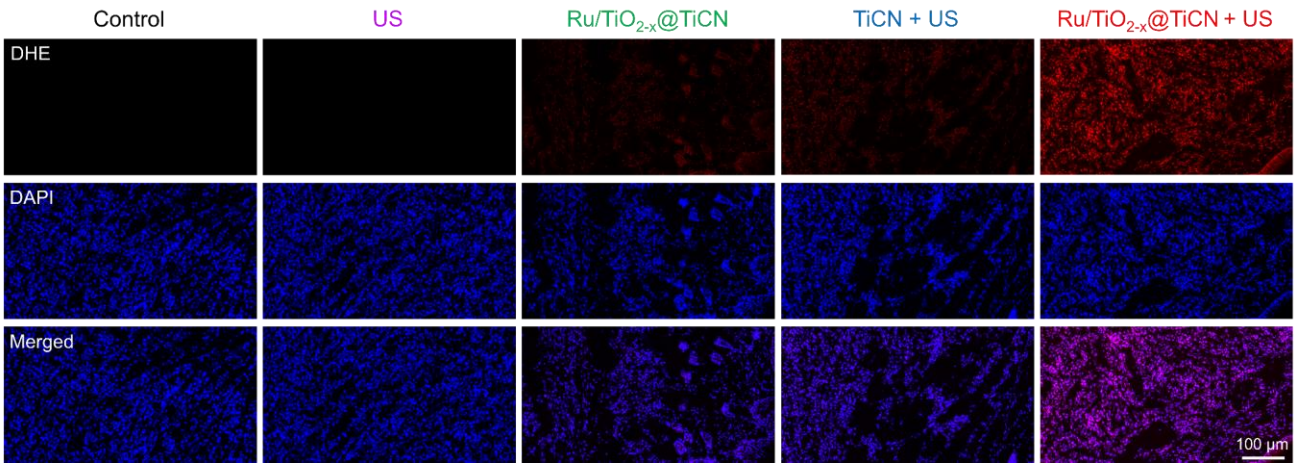

Figure S23. ROS staining of tumors in mice after different treatments.

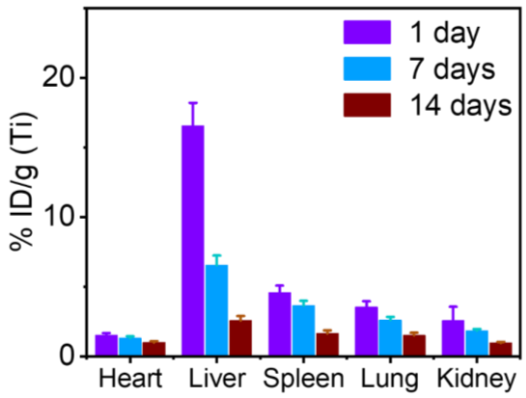

Figure S24. Biodistribution of Ru/TiO_{2-x}@TiCN post i.v. injection in mice on different days (1, 7, and 14 days) (n=5).

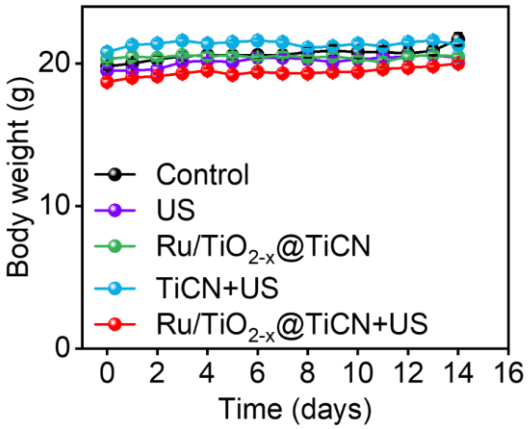

Figure S25. Body weight curves of the treated mice after different treatments (n=5).

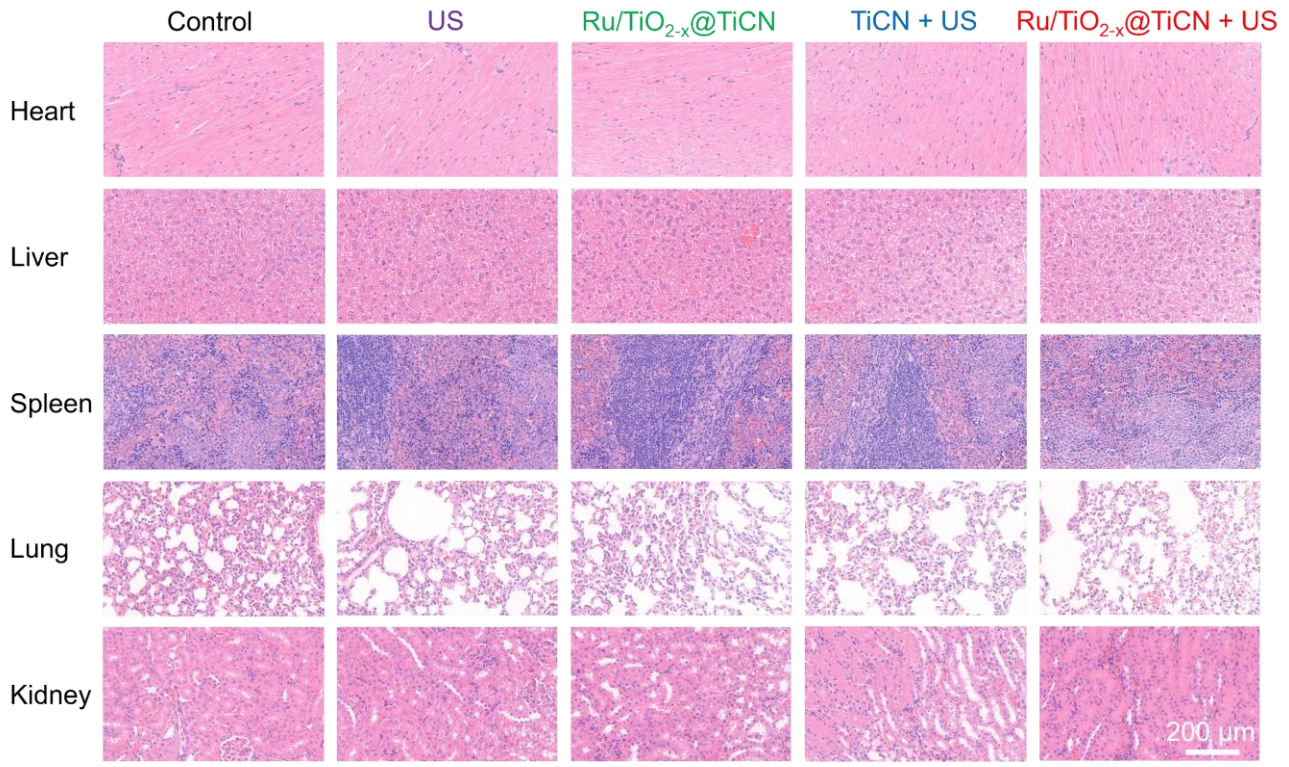

Figure S26. H&E-stained images obtained from the major organs (heart, liver, spleen, lung, and kidney) of mice in different treatment groups.

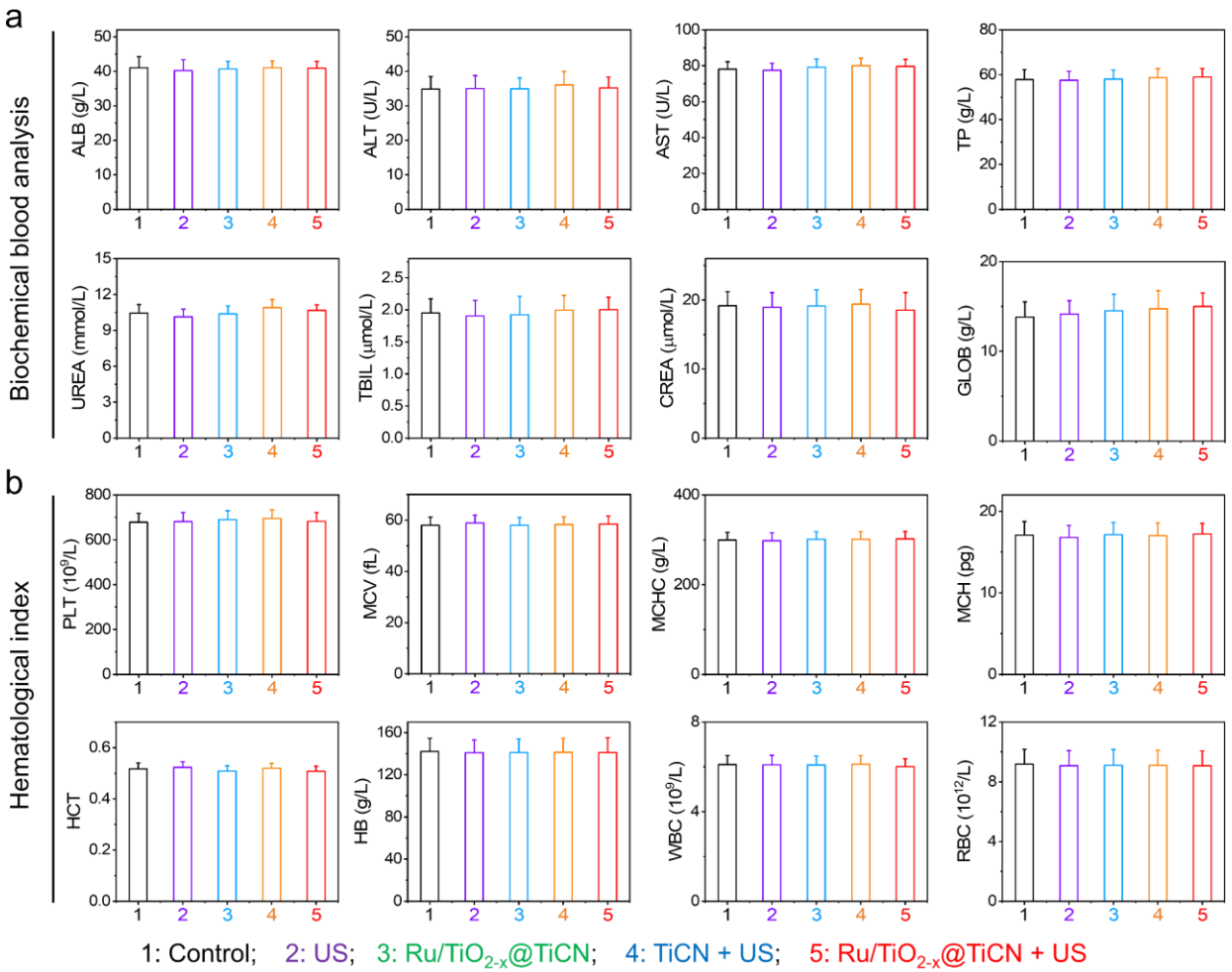

Figure S27. (a-b) Biochemical blood analysis (a) and hematological index (b) of the mice that were sacrificed at 18 days after different treatments (n=5).